Siberian trap magmatism on the New Siberian Islands: constraints for Arctic Mesozoic plate tectonic reconstructions

Alexander B. Kuzmichev and Victoria L. Pease

Journal of the Geological Society 2007; v. 164; p. 959-968
doi:10.1144/0016-76492006-090

Journal of the Geological Society, London, Vol. **164**, 2007, pp. 959–968. Printed in Great Britain.

Siberian trap magmatism on the New Siberian Islands: constraints for Arctic Mesozoic plate tectonic reconstructions

ALEXANDER B. KUZMICHEV[1] & VICTORIA L. PEASE[2]

[1]*Geological Institute of the Russian Academy of Sciences, Pyzhevsky 7, 119017 Moscow, Russia (e-mail: kuzmich@ilran.ru)*

[2]*Department of Geology and Geochemistry, Stockholm University, Stockholm SE-106 91, Sweden*

Abstract: It is widely held that a large composite terrane including the East Siberian shelf, Northern Chukotka and Arctic Alaska moved to its current location from the other side of the Mesozoic ocean in the course of the Amerasia basin opening. The western boundary of this terrane is critical for tectonic models of the Mesozoic Arctic. Consequently, the New Siberian Islands, which lie in the centre of this critical region, should help to define the position of this boundary. We have studied subvolcanic gabbroic intrusions on Bel'kov Island, the westernmost island in the New Siberian Archipelago. Their age is 252 ± 2 Ma (U–Pb zircon, secondary ion microprobe technique) and they represent mantle-derived tholeiitic magma modified by continental crust contamination. Their age and petrographic and geochemical features are identical to those of the Siberian traps, suggesting that in Early Mesozoic time the western New Siberian Islands were adjacent to northern Siberia (modern coordinates). This indicates that the large composite terrane that includes the western New Siberian Islands is not exotic to Siberia as is currently implied in some Arctic Mesozoic tectonic reconstructions.

The New Siberian Islands separate the Laptev and East Siberian Seas, which occupy the Eastern Arctic shelf (Fig. 1). The Laptev Sea shelf was affected by extensive stretching to compensate for the spreading of the Eurasia oceanic basin. Its recent structure is controlled by a rift system initiated in Late Cretaceous time (e.g. Drachev *et al*. 1998). The structure of the pre-Late Cretaceous basement is poorly revealed by geophysical data and is almost unknown. The East Siberian Sea shelf is less disrupted by young rifts. Most of this area represents a continental terrane with Late Precambrian metamorphic basement and a Palaeozoic cover of mainly carbonate rocks (Kos'ko *et al*. 1985, 1993; Natal'in *et al*. 1999). Most workers combine the East Siberian shelf, Northern Chukotka and Arctic Alaska into a composite terrane that rifted from Arctic Canada, rotated counterclockwise and accreted to NE Asia in the Early Cretaceous during the opening of the Amerasia basin (Fig. 1) (e.g. Rowley & Lottes 1988; Grantz *et al*. 1998; Lawver *et al*. 2002). It is commonly accepted that the South Anyui suture bounds this terrane to the south (Fig. 1) (e.g. Natal'in *et al*. 1999; Sokolov *et al*. 2002).

The location of the western boundary of this terrane is highly controversial. The easternmost location (line 1, Fig. 1) was suggested by Rowley & Lottes (1988). This was an attempt to provide a geometrical solution for a kinematic problem arising from the rotational hypothesis for the opening of the Amerasia basin. No geological or geophysical evidence is known indicating that the South Anyui suture ends near the Kolyma River mouth. Other reseachers have placed this controversial boundary further to the west (line 2, Fig. 1) (e.g. Parfenov *et al*. 1993; Layer *et al*. 2001). This solution attempts to reconcile the rotational hypothesis and the fact that the South Anyui suture extends westward to Big Lyakhov Island (Fig. 2). This implies that the South Anyui suture turns north from Big Lyakhov Island and passes through the Anjou Islands. However, the geological data are not consistent with this idea. No obvious indications of the suture, such as oceanic or island-arc rocks, have been found in the area. The precollision Jurassic deposits on all of the Anjou Islands are weakly deformed non-lithified shallow marine clays (Kos'ko *et al*. 1985; Trufanov *et al*. 1986, and the authors' data). The next proposed location for this boundary is west of the New Siberian Islands (line 3, Fig. 1). This is the only location that is supported by geological evidence. Mapping of Bel'kov Island has revealed structural features that could be related to a north–south dextral transform (Kuzmichev & Bogdanov 2003). A similar location for this boundary was suggested by Drachev *et al*. (1998), who placed the South Anyui suture west of Bel'kov Island, and by Natal'in *et al*. (1999), who interpreted Kotel'ny Island, the East Siberian shelf and Wrangel Island as the intact Bennett–Barrovia block. However, they also showed a NW branch of the South Anyui suture passing between Bunge Land and Faddeev Island (Natal'in *et al*. 1999, figs 7 and 9). This third solution is not compatible with the rotational hypothesis. It is evident that if line 3 (Fig. 1) is accepted as the western border of the rotated terrane, it is too large to fit the Arctic Canada margin (Fig. 1). A fourth option was suggested by Zonenshain *et al*. (1990), who combined the East Siberian shelf, New Siberian Islands, northern Taimyr and Severnaya Zemlya into the 'Arctida' palaeocontinent. The Arctida hypothesis was also implied by Sokolov *et al*. (2002), as well as others. It is obvious that Arctida is inconsistent with a plane rotational opening for the Amerasia basin.

Thus, the location of this western tectonic boundary is of great importance for tectonic models of Early Mesozoic Arctic evolution. The New Siberian Islands occur in the centre of this controversial area, and their investigation should contribute to resolving this issue. The archipelago consists of three groups of islands (Fig. 2). The Lyakhov Islands are composed of deformed Upper Jurassic–Lower Cretaceous terrigenous deposits accumulated within a syncollisional foreland basin (Kuzmichev *et al*. 2006). The western Anjou Islands are composed of Palaeozoic platformal rocks. The eastern Anjou Islands are covered with Mesozoic and Cenozoic continental deposits. The northernmost part of the archipelago (Zhannette and Henrietta Islands or the entire De Long Islands territory) presumably represents a differ-

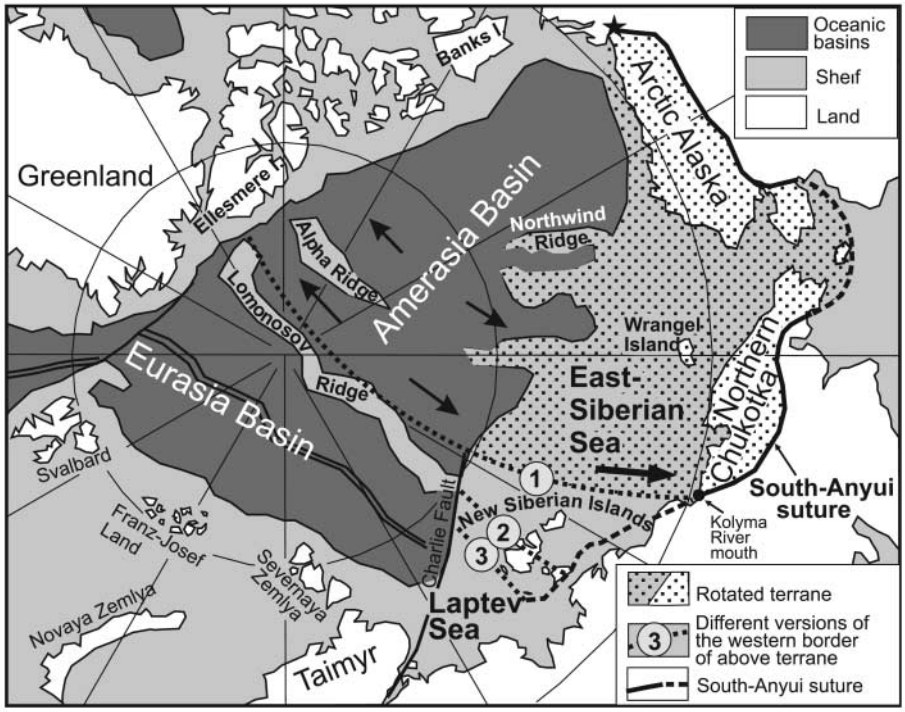

Fig. 1. A general view of the Arctic region showing the location of the New Siberian Islands. In the context of the rotational hypothesis for the opening of the Amerasia basin, the dotted area outlines the rotated terrane that has presumably drifted away from Arctic Canada around a pole of rotation indicated by the star. The position of the western boundary of this terrane is controversial. Three models for the location of this terrane boundary are indicated: (1) after Rowley & Lottes (1988); (2) after Spector *et al*. (1981) and Parfenov *et al*. (1993); (3) after Kuzmichev & Bogdanov (2003).

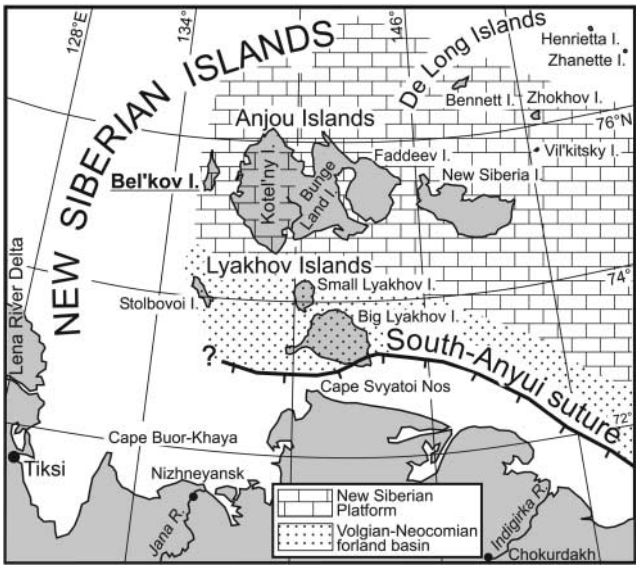

Fig. 2. General geological setting of the New Siberian Islands. Most of the region was designated as Palaeozoic carbonate platform (Natal'in *et al*. 1999). The southern portion of the archipelago represents Mesozoic foreland basin filled with Late Jurassic–Neocomian flysch (Kuzmichev *et al*. 2006). The position of the South Anyui suture is shown after Kuzmichev *et al.* (2005, 2006). These features all trend towards Northern Chukotka.

ent terrane (Natal'in *et al*. 1999; Vol'nov *et al*. 1999; Kos'ko & Trufanov 2002), which is beyond the scope of this paper.

Kotel'ny and Bel'kov islands (Fig. 2) are most informative for possible geological correlation with westward- and eastward-lying terranes, as they expose an almost complete succession of Palaeozoic deposits (Kos'ko *et al*. 1985). These deposits were described by Natal'in *et al*. (1999) as the New Siberian carbonate platform, which extends beyond Wrangel Island as far east as Alaska. However, Cherkesova (1975) suggested that the Kotel'ny Palaeozoic rocks and fossils are similar to those of southern Taimyr. Thus, more convincing arguments are required to make reliable correlations and to constrain Mesozoic Arctic tectonic evolution.

At the Permian–Triassic boundary the Siberian Platform and adjacent areas experienced significant basaltic intraplate igneous activity (e.g. Renne & Basu 1991; Kamo *et al*. 2003; Dobretsov 2005). Numerous doleritic and gabbroic bodies with similarities to Siberian trap dolerites have been found on Bel'kov Island (Kuzmichev 2004). Samples were collected for age and geochemical analyses to test whether a correlation might exist between magmatism occurring on the western Anjou Islands and the northern Siberian Platform. Our analytical results indicate that the western New Siberian Islands were a part of the Siberian trap province, thus they formed a continuous landmass with the Siberian Platform in the Early Triassic. This conclusion has important implications for Arctic tectonic reconstructions, as it contradicts the common opinion that the terrane that includes the New Siberian carbonate platform is exotic to Siberia and rotated to its present position after rifting from Arctic Canada (Zonenshain *et al*. 1990; Drachev *et al*. 1998; Natal'in *et al*. 1999; Sokolov *et al*. 2002).

Geological setting

Bel'kov Island is composed of Palaeozoic carbonate and terrigenous rocks (Kos'ko & Nepomiluev 1980). Type-sections of these units occur on Kotel'ny Island, where similar deposits are highly fossiliferous and gently deformed (Kos'ko *et al*. 1985). Bel'kov Island was mapped using the same stratigraphic units as on Kotel'ny Island. We recognize only three main lithostratigraphic units on the island, partly conforming to the subdivision by

Kos'ko & Nepomiluev (1980): (1) Middle Devonian shelf carbonates (the Sokolov Fm); (2) Late Devonian–Tournaisian light grey platy siltstones, sandstones, carbonate conglomerates and olistostrome (the Nerpalakh and Chekurskaya Fms); (3) Carboniferous–Permian sandstones and black shales with siderite concretions (the Bel'kov Fm) (Fig. 3). The unfossiliferous Bel'kov Formation was inferred to be Middle Carboniferous in age, as it was lithologically similar to the Bashkirian deposits on Kotel'ny Island (Kos'ko *et al*. 1985). However, the results of our study show that the Palaeozoic section on Bel'kov Island is continuous and the Bel'kov Formation includes Early to Late Carboniferous and probably Permian deposits as well. Palaeozoic rocks were folded, faulted and cleaved to different degrees. This deformation is inferred to have occurred in Neocomian time from the unconformity between Upper Jurassic and Aptian deposits on Kotel'ny Island (Kos'ko *et al*. 1985).

Numerous dolerite and gabbro–dolerite intrusions are recognized on Bel'kov and western Kotel'ny Islands (Kos'ko & Nepomiluev 1980; Kuzmichev 2004). They were presumed to be mid-Palaeozoic in age by Kos'ko *et al*. (1985); however, on Bel'kov Island dolerites intrude the entire section including the Late Palaeozoic Bel'kov Fm. (Fig. 3). The intrusions form clusters, which are interpreted as subvolcanic centres (Kuzmichev 2004). A north–south volcanic chain presumably extended along western Bel'kov Island. Separate dykes are also scattered over the rest of the island. Similar intrusions frequently occur in the southwestern part of Kotel'ny Island (Kos'ko *et al*. 1985). A 1:200 000-scale aeromagnetic survey (by NIIGA in 1973–1974) revealed major magnetic anomalies on Kotel'ny and Faddeev Islands and on the adjacent shelf, which may indicate subsurface gabbroic bodies, belonging to the same suite as on Bel'kov Island.

Igneous rocks, occurrence and petrography

Most of Bel'kov Island is poorly exposed, but as seen in cliffs, igneous rocks form dykes, stocks and irregular bodies (Fig. 4). At places they dominate volumetrically the Palaeozoic host sediments. The structural orientation of the intrusions is usually unrelated to sediment layering. This is true for Late Devonian and especially for Carboniferous–Permian sediments, which provided a nearly isotropic soft substrate during the emplacement of basaltic magma.

Fragmental igneous rocks include vent hyaloclastite, peperite and eruptive(?) breccia. The origin of the breccias is not known, but they may represent a diatreme. Such igneous bodies occur only in shales of the Bel'kov Formation, the youngest Palaeozoic strata on Bel'kov Island.

The textures of typical rocks vary from glassy and microlitic in the fragmental rocks and thin dykes, to porphyritic or ophitic in small bodies, poikilophitic in larger bodies, and gabbroic in large massifs. The glassy matrix in fine-grained rocks is completely replaced by secondary minerals. Dolerites are generally composed of euhedral plagioclase, anhedral clinopyroxene, and rare olivine. In poikilophitic varieties, brownish clinopyroxene makes up 0.5–1.5 cm oikocrysts with plagioclase laths. Interstices are filled with hornblende, chlorite, some biotite, apatite and ore minerals. In phyric varieties there occur several generations of plagioclase: large zoned phenocrysts, short laths and long microlites. Olivine is pseudomorphed by chlorite. Some samples contain sphene.

Picrite dykes that cut gabbro–dolerite bodies were found on Cape Polundra (Fig. 3). The dykes contain about 15% fresh euhedral olivine phenocrysts with fayalitic low-temperature rims.

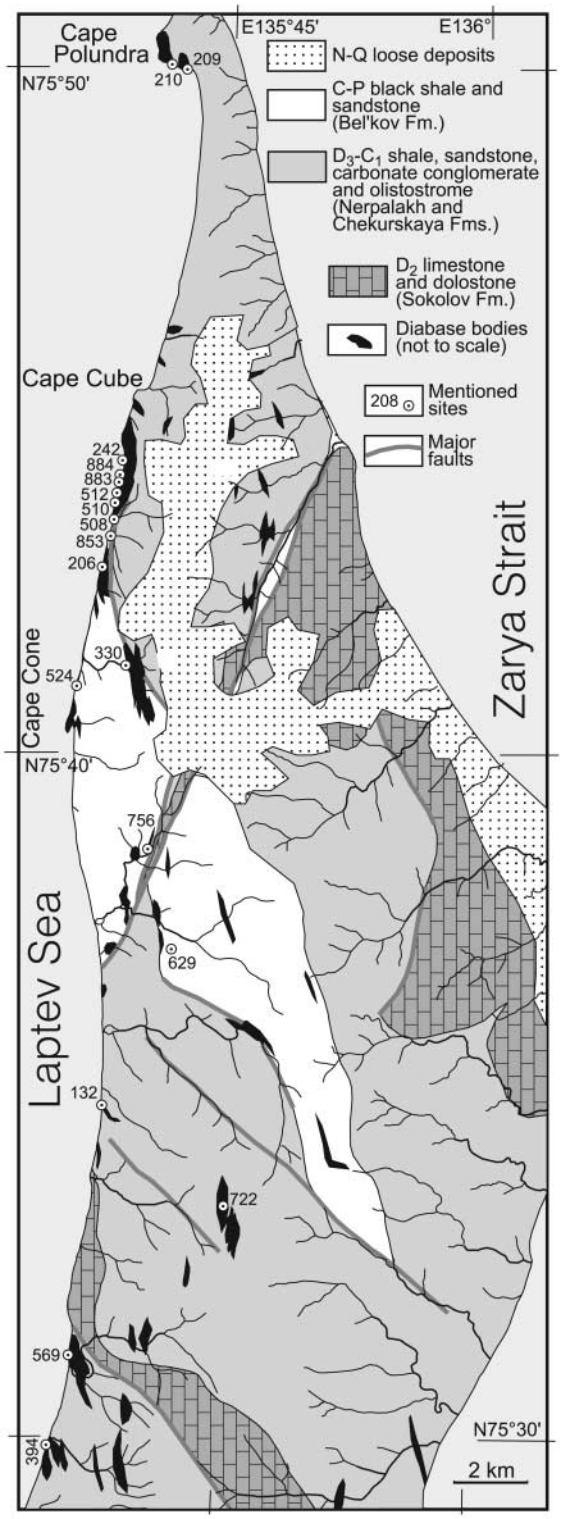

Fig. 3. Geological map of the studied portion of Bel'kov Island, based on the 2002 and 2004 field studies. The unit ages are from Kos'ko *et al*. (1985) and our unpublished data. The size of most igneous bodies has been exaggerated to be visible at this scale.

The most leucocratic rock occurs at site 512 (Fig. 4) and is a medium-grained, highly carbonatized rock composed of plagioclase, K–Na feldspar, chlorite and quartz. Large gabbro–dolerite bodies sometimes show gabbro–pegmatite schlieren consisting

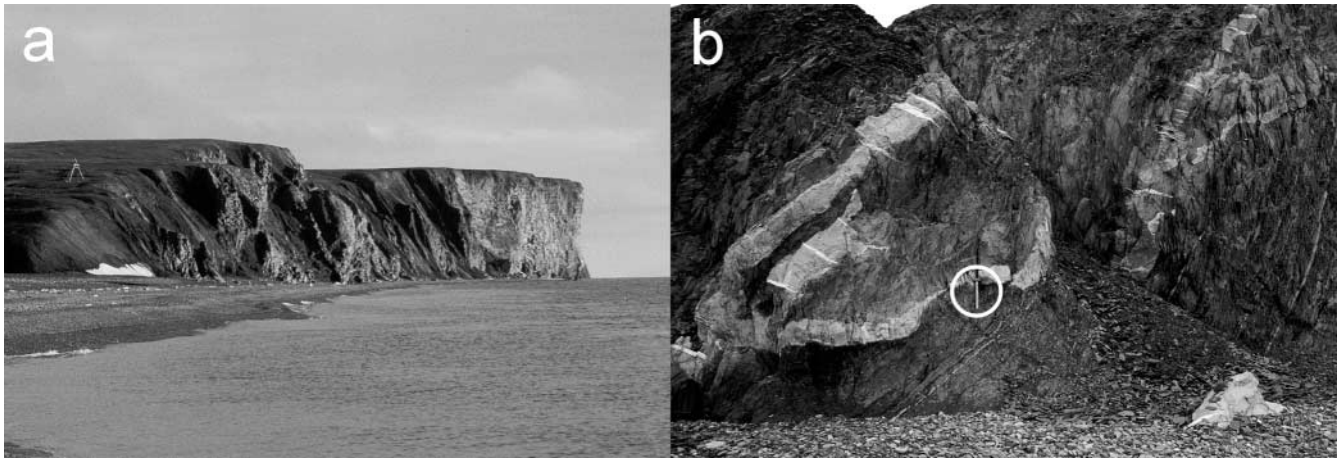

Fig. 4. Typical dolerite outcrops in the western cliff of Bel'kov Island. Site numbers are given in Figure 3. (**a**) A set of numerous dykes and a large stock (at the far end) in a cliff between sites 853 and 206. Light-coloured hard rock is dolerite, dark-coloured soft rock is host black shale. The cliff's distant part is 50 m high. A southward view from site 508. (**b**) Branching dolerite dyke (site 132). The host Nerpalakh strata were unconsolidated at the time of intrusion. The hammer indicates scale.

of oligoclase, which passes into granophyre, large (several centimetres) hornblende crystals and chlorite. Syenite schlieren were also reported in the gabbro massif outside our study area in the southeastern part of the island (Kos'ko *et al*. 1985). Minor dykes and dolerite fragments in breccias are highly carbonatized.

We interpret most of the peperitic or brecciated igneous bodies to be subsurface intrusions. Nevertheless, some of them (e.g. sites 242, 330, Fig. 3) may actually represent fragmental tuffs. Basaltic lava presumably occurs on the island as well. Highly vesicular basaltic fragments are sometimes found in poorly exposed locations (e.g. site 629, Fig. 3). The lava-resembling varieties occur around site 206 (Fig. 3). The host rocks in these localities belong to the Bel'kov Formation.

The age of magmatism

Most of the Bel'kov intrusions were originally interpreted as Middle Palaeozoic in age (Kos'ko *et al*. 1985). This seemed reasonable, as mafic Late Devonian intrusions were widespread along the eastern Siberian Platform, particularly in the Lena Delta region (Prokopiev *et al*. 2001). However, dolerite textures, and especially the pisolitic-like habit of Bel'kov poikilophitic varieties, are similar to those of sills related to the Siberian traps that are observed throughout the Siberian Platform from the Angara River in the south to Pyasina River in the north (e.g. Unksov 1934; Sheinman 1947). This similarity became obvious during fieldwork, thus it was especially important for us to determine the true age of Bel'kov dolerites. Samples were collected from highly evolved pegmatitic and leucocratic rocks because these were more likely to contain zircon for U–Pb dating. However, high-quality zircon crystals were obtained only from the biotite-gabbro–dolerite sample 210/3 from Cape Polundra (Fig. 3).

Analytical method and results

Zircons were analysed by U–Th–Pb using a Cameca IMS1270 ion-microprobe at the NORDSIM facility in Stockholm. Methods for sample preparation and analytical procedures follow those described by Whitehouse *et al*. (1997, 1999). The data are corrected for common lead using the model lead composition of Stacey & Kramers (1975), anchored to 0 Ma. Because of the small ion-beam size (*c*. 25 μm) and relatively low lead counts, the ^{207}Pb-corrected age is reported for all analyses.

Ten grains were analysed from sample 210/3 (Table 1). The data define a relatively well-grouped concordant cluster, with 9/10 grains within error of each other (Fig. 5). The corrected data yield a nine-point concordia age of 252 ± 2 Ma (95% confidence, MSWD $= 1.3$, $n = 9$), which is interpreted as the time of crystallization. These data refute a Mid-Palaeozoic age for the majority of Bel'kov Island igneous rocks (Kos'ko *et al*. 1985) and indicate that they were emplaced synchronously with Siberian traps.

Correlation with the age of Siberian traps

It is broadly accepted that a huge volume of Siberian traps erupted during a very short time interval at the Permian–Triassic boundary, dated at 251–252 Ma (see discussion by Kamo *et al*. 2003). This magmatic episode is considered to be the most catastrophic event in the Earth's Phanerozoic history (Renne & Basu 1991), and a mass extinction at the end of the Permian may have been caused by volcanic activity associated with Siberian trap emplacement (Renne *et al*. 1995; Benton & Twitchett 2003). Thus, it was important to determine the age and duration of igneous activity associated with Siberian traps, and a large array of age data has now been accumulated. Most of the available ^{40}Ar/^{39}Ar dates group at around 250 Ma and mostly lie within the error limits of each other (Dalrymple *et al*. 1995; Venkatesan *et al*. 1997; Reichow *et al*. 2002). More precise ages were obtained by U–Pb dating using the thermal ionization mass spectrometry (TIMS) technique for single- and multi-grain zircon, perovskite and baddeleyite (Kamo *et al*. 1996, 2003). The onset of Siberian trap volcanism in the northern Siberian Platform was dated at 251.7 ± 0.4 Ma. An age of 251.1 ± 0.3 Ma was obtained from the upper part of volcanic sequence. Termination of volcanic activity was dated at 250.2 ± 0.3 Ma by carbonatite intruding the upper volcanic series. These age data constrain the entire trap emplacement record to a very short time period. Our data are within error of the time of flood-basalt

Table 1. *U–Th–Pb ion-microprobe analytical data from gabbro of Bel'kov Island*

Grain no.	U (ppm)	Th (ppm)	Pb (ppm)	Th/U	f_{206} (%)	$^{207}Pb/^{206}Pb$	±1σ%	$^{238}U/^{206}Pb$	±1σ%	Disc. (2σ)%	$^{207}Pb/^{206}Pb$ corrected		$^{206}Pb/^{238}U$ corrected	
											Age (Ma)	±1σ	Age (Ma)	±1σ
1	311	276	16	0.887	0.16	0.04993	1.53	25.302	1.17		192	35	250	3
2	701	1282	45	1.829	0.05	0.05094	1.04	24.905	1.17		238	24	254	3
3	171	152	9	0.886	0.24	0.04811	2.25	25.251	1.17		105	52	250	3
4	509	733	31	1.440	0.16	0.04991	1.20	24.805	1.19	1.1	191	28	255	3
5	251	239	13	0.955	0.12	0.04983	1.65	24.879	1.19		187	38	254	3
6	248	203	13	0.816	0.32	0.04958	1.98	25.279	1.19		176	46	250	3
7	246	253	13	1.028	0.10	0.05132	1.49	25.003	1.18		255	34	253	3
8	434	791	28	1.824	0.13	0.05098	1.26	24.863	1.19		240	29	254	3
9	425	429	23	1.010	0.19	0.04991	1.37	25.013	1.17		191	32	253	3
10	228	203	12	0.892	0.24	0.04968	2.39	25.022	1.17		180	55	253	3

Analyses were performed on a high mass resolution, high-sensitivity Cameca IMS 1270 ion-microprobe at the NORDSIM facility in Stockholm. Th/U ratios from measured ThO/U calibrated to the standard. f_{206}(%), fraction of common Pb calculated from ^{204}Pb. Data are reported at 1σ. All ages are calculated using the decay constants of Steiger & Jäger (1977). Disc., degree of discordance at the 2σ error limit between $^{207}Pb/^{206}Pb$ and $^{206}Pb/^{238}U$ ages; reverse discordance is indicated by positive numbers. Errors in age estimate are quoted at 1σ. Pb concentrations determined after correction for common Pb. Corrected ages calculated assuming common Pb composition after Stacey & Kramers (1975).

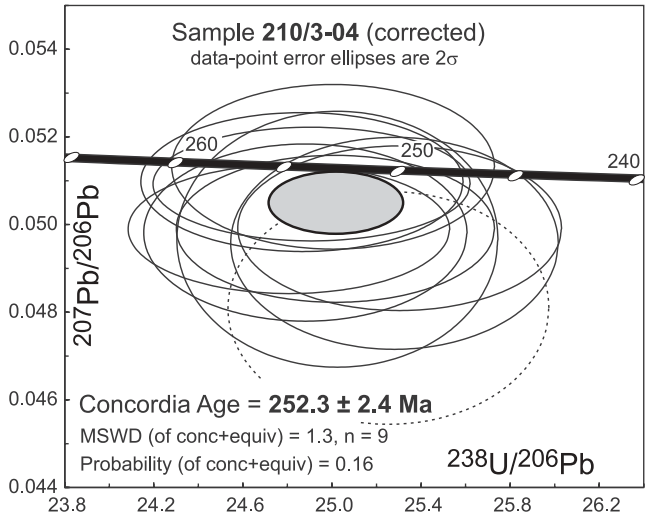

Fig. 5. Inverse concordia diagram for gabbro 210/3-04 from northern Bel'kov Island. The age is reported at the 95% confidence limit. Sample location is 75°50′03.7″N, 135°41′27.5″E.

volcanism and suggest that the mafic intrusions of Bel'kov Island may represent the Siberian trap magmatism.

Chemical composition

The intraplate tectonic setting of mafic intrusions on Bel'kov Island, occurring in platformal deposits, is obvious from geological data. Therefore, we use geochemical data, not to define the tectonic environment, but rather to verify the suggested correlation of these rocks with Siberian traps. The Bel'kov Island igneous rocks represent evolved mantle-derived magma of basaltic composition (Mg − number = 0.38–0.58; SiO_2 47.6–52.0% for common rocks) (Table 2). The rocks contain moderate TiO_2 (1–2%) and MgO (4–8.5%), high $Fe_2O_3^T$ (10.6–15.8%), low or moderate Al_2O_3 (13–17.5%) and relatively high K_2O (up to 1.8%, average 0.9%). Some rocks containing K-feldspar are probably alkaline, but they were not analysed because of carbonatization. The most primitive rock (sample 209/2, Mg − number = 0.64) is picritic porphyry with high MgO and $Fe_2O_3^T$. Most samples are classified as tholeiites in terms of MgO/FeO ratio and Al_2O_3 content. The Bel'kov Island igneous rocks are variously enriched in light rare earth elements (LREE), (La/Yb(n) = 2.1–9.2). The complementary negative and positive Eu anomalies (Table 2) imply *in situ* plagioclase fractionation. Most samples show enrichment in large ion lithophile elements (LILE) including Rb, Ba and K, as well as depletions in Nb and Ta (Th/Nb = 0.13–0.73) (Table 2).

These features are typical of Siberian traps (Reichow *et al*. 2005). Average values of Siberian trap compositions are taken from Al'Mukhamedov *et al*. (1999), who recognized two predominant magmatic types: 'low-K tholeiites' and 'subalkaline basalts'. For comparison we have also subdivided our samples into two groups: (1) those with high La/Yb(n) values (5.3–6.2); (2) those with relatively low La/Yb(n) values (2.1–3.4). Average compositions were calculated excluding exotic rocks (samples 209/2 and 883/1). However, these two groups are not direct analogues of the two Siberian basaltic suites, as a lower La/Yb ratio in some Bel'kov dolerites could be caused by the abundance of cumulus phases.

Comparison of Bel'kov dolerites and Siberian trap basalts indicates their overall geochemical similarity. The REE patterns of the high La/Yb and low La/Yb groups of Bel'kov dolerites resemble those of the 'subalkaline' and 'tholeiitic' suites of Siberian traps, respectively, and differ from them in their lower concentrations of all REE (Fig. 6a). Other trace element concentrations in Bel'kov rocks are also similar to those of Siberian basalts (with the exception of Sr content), and resemble those of the subalkaline suite (Fig. 6b). Both diagrams demonstrate obvious differences between continental traps (including Siberian and Bel'kov ones) and oceanic basalts (including ocean island basalt (OIB) and mid-ocean ridge basalt (MORB)). This difference is most evidently manifested by negative Nb anomalies and positive LILE spikes in Siberian traps and Bel'kov dolerites (Fig. 6b). The Th/Nb v. Ba/La diagram (Fig. 7) best illustrates these differences. However, negative Nb anomalies, and the LILE and LREE enrichment, are also commonly regarded as indicating 'island-arc' geochemical affinity. Furthermore, similar features are also typical of some continental flood basalts (Hergt *et al*. 1991; Peate & Hawkesworth 1996; Pik *et al*.

Table 2. *Chemical composition of the Bel'kov Island dolerites*

Sample:	510/1	524/2	569/2	569/5	722/1	756/1	883/1	884/1	209/2	210/3	394/1
SiO_2	49.81	49.86	48.53	48.68	46.71	50.89	54.78	49.22	45.26	47.60	48.03
TiO_2	0.99	1.13	1.04	1.89	2.13	1.04	1.23	0.96	1.33	1.82	1.83
Al_2O_3	15.10	16.05	14.89	17.31	15.19	15.81	13.66	14.99	11.19	12.83	12.81
$Fe_2O_3^T$	11.43	10.46	11.28	13.00	14.79	10.38	14.13	10.70	16.59	15.08	15.52
MnO	0.20	0.17	0.18	0.18	0.20	0.19	0.21	0.19	0.19	0.20	0.19
MgO	7.52	6.93	8.34	3.98	5.22	6.67	3.67	7.41	14.51	8.19	7.72
CaO	9.15	10.35	12.83	9.85	10.13	8.64	4.05	10.26	5.72	10.39	9.75
Na_2O	2.19	1.68	1.76	2.88	2.72	2.21	4.24	2.26	1.63	1.80	1.53
K_2O	0.73	0.62	0.33	0.88	0.83	1.73	0.73	1.34	0.87	0.67	0.63
P_2O_5	0.16	0.20	0.15	0.20	0.21	0.21	0.20	0.17	0.24	0.21	0.21
LOI	2.78	2.64	0.72	1.18	1.93	2.27	3.15	2.55	2.55	1.27	1.83
Sum	100.05	100.09	100.02	100.03	100.05	100.04	100.04	100.06	100.09	100.05	100.05
Mg-no.	0.57	0.57	0.60	0.38	0.41	0.56	0.34	0.58	0.64	0.52	0.50
Sc	33	37	48	30	38	33	27	33	13	30	32
Rb	28	16	9.5	52	28	51	30	62	18	18	20
Sr	288	263	177	276	288	476	273	539	430	290	218
Y	24	28	18	30	24	22	34	23	25	29	29
Zr	92	93	41	61	65	105	137	91	84	96	64
Nb	5.5	7.8	2.6	6.0	5.0	8.0	6.4	6.1	2.0	2.2	5.0
Cs	1.1	1.5	0.92	4.0	1.2	2.1	1.8	2.3	4.1	1.6	6.8
Ba	363	385	78	155	373	3160	267	805	386	350	258
La	13.2	14.3	4.08	8.45	7.60	14.6	29.6	13.7	21.8	10.3	9.25
Ce	28.0	28.3	9.71	19.0	17.9	29.0	58.1	27.5	41.6	22.3	20.2
Pr	3.7	3.8	1.5	2.7	2.5	3.9	7.1	3.5	5.5	3.2	2.8
Nd	15.0	14.8	6.55	11.7	10.8	14.3	26.7	13.4	21.5	14.6	12.9
Sm	3.63	3.55	2.01	3.17	3.11	3.43	5.43	3.24	4.83	3.98	3.58
Eu	0.92	1.1	0.85	1.3	1.3	1.4	1.2	1.0	1.5	1.4	1.2
Gd	3.63	3.38	2.55	3.63	3.29	3.24	5.13	3.47	4.36	4.21	3.90
Tb	0.56	0.56	0.43	0.60	0.51	0.52	0.78	0.52	0.73	0.75	0.72
Dy	3.46	3.38	2.61	3.59	3.25	3.00	4.58	3.23	3.97	4.22	4.20
Ho	0.78	0.74	0.60	0.81	0.70	0.65	0.98	0.68	0.76	0.85	0.86
Er	1.9	1.8	1.5	2.0	1.7	1.7	2.5	1.7	2.1	2.2	2.4
Tm	0.29	0.28	0.22	0.31	0.25	0.26	0.38	0.25	0.29	0.34	0.36
Yb	1.8	1.7	1.4	1.8	1.6	1.7	2.5	1.6	1.7	2.0	2.1
Lu	0.26	0.24	0.20	0.29	0.25	0.26	0.36	0.25	0.26	0.29	0.29
Hf	1.83	1.76	0.96	1.06	1.34	1.98	2.71	1.84	1.75	1.82	1.62
Ta	0.35	0.43	0.18	0.29	0.36	0.45	0.47	0.38	0.38	0.29	0.58
Pb	6.61	4.83	1.38	1.87	9.94	3.72	4.71	9.17	6.02	3.13	0.84
Th	1.66	1.72	0.41	0.84	0.66	2.13	3.82	1.83	1.45	0.88	0.98
U	0.59	0.45	0.14	0.25	0.29	0.61	0.79	0.48	0.40	0.24	0.39
Eu_n/Eu^*	0.77	0.97	1.15	1.17	1.24	1.28	0.70	0.91	1.00	1.05	0.98
La/Yb(n)	5.3	6.0	2.1	3.4	3.4	6.2	8.5	6.1	9.2	3.7	3.2
La/Sm(n)	2.3	2.6	1.3	1.7	1.6	2.7	3.5	2.7	2.9	1.7	1.7
Gd/Yb(n)	1.7	1.6	1.5	1.7	1.7	1.6	1.7	1.8	2.1	1.7	1.5
Th/Nb	0.30	0.22	0.16	0.14	0.13	0.27	0.60	0.30	0.73	0.40	0.20
Ce/Nb	5.09	3.63	3.73	3.17	3.58	3.63	9.08	4.51	20.80	10.14	4.04

Major oxides in wt%; trace elements in ppm; LOI, loss on ignition. Location of samples is shown in Figure 3. Major element data were obtained on fused pellets by XRF at the UIGGM (Novosibirsk). Detection limits: 0.2 for Na_2O; 0.1 for MgO; 0.05 for SiO_2; 0.02–0.005 for others. REE and trace elements were determined by inductively coupled plasma mass spectrometry at the Limnological Institute (SB RAS, Irkutsk). The instrument configuration, operating conditions, and sample dissolution technique are after Garbe-Schonberg (1993). Calibrations were set using internal standards and international rock standards (BHVO-1, BIR-1, W-2, RGM-1). Precision and accuracy are about 5%. Samples 510/1, 524/2, 569/2, 569/5, 722/1, 756/1 and 884/1 are ophitic–poikilophitic dolerite; sample 394/1 is gabbro–dolerite; 210/3 is Bi-gabbro–dolerite; 209/2 is Ol-picritic dyke; 883/1 is pegmatite. Mg – number = $MgO/(MgO + FeO^T)_{mol}$; $Eu^* = (Sm_n \times Gd_n)^{1/2}$ (where subscript n indicates chondrite-normalized).

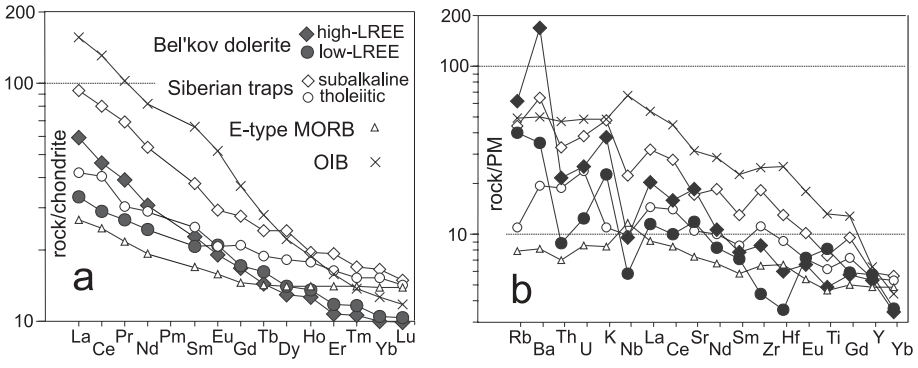

Fig. 6. REE and multi-element diagrams for comparison of Bel'kov dolerites with Siberian trap basalts, OIB and E-MORB. Normalizing values, incompatible element order and data for OIB and E-MORB are after Sun & McDonough (1989). Data for Siberian traps are after Al'Mukhamedov *et al*. (1999). E-MORB, enriched mid-oceanic ridge basalts; PM, primitive mantle.

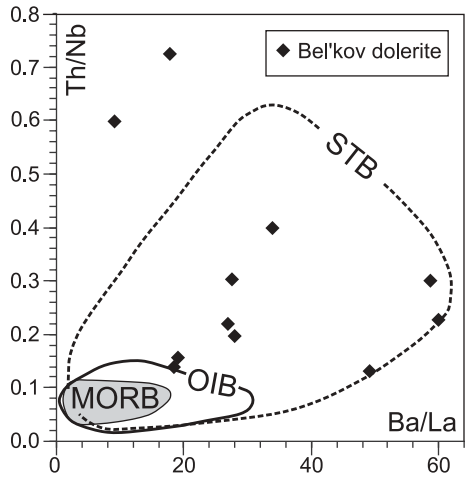

Fig. 7. Ba/La v. Th/Nb plot. The Bel'kov dolerites are enriched with Ba and Th similar to Siberian traps (STB contour) in comparison with oceanic basalts (OIB and MORB fields). The data for MORB, OIB and STB were obtained from the PETDB (http://www.petdb.org/) and GEOROC (http://georoc.mpch-mainz.gwdg.de/georoc/) databases. The MORB field is outlined by the Mid-Atlantic Ridge basalts; the OIB field by the Hawaiian Islands basalts; the STB field by the Siberian trap basalts and dolerites.

1999) and of Siberian traps in particular (Lightfoot *et al*. 1990, 1993; Sharma *et al*. 1991, 1992; Wooden *et al*. 1993; Hawkesworth *et al*. 1995; Reichow *et al*. 2005). These features are usually attributed to contamination of mantle-derived magma by continental crust material (Arndt *et al*. 1993, and most of the above-cited studies) or to remelting of subcontinental lithospheric upper mantle modified by subduction-related processes at earlier stages of lithosphere formation (e.g. Walker *et al*. 1994).

Thus, the geochemical data permit us to attribute the Bel'kov Island intrusions to continental flood basalt magmatism and, in particular, to the Siberian trap varieties characterized by elevated alkalinity. As we shall see below, such rocks are most common in the northern Siberian trap province.

The position of the Bel'kov igneous suite in the Siberian trap province

The manifestation of Bel'kov Island mafic magmatism is similar to that exposed on Taimyr Peninsula and both probably lie within the northern limits of the Siberian trap province (Fig. 8). In southern Taimyr, trap magmatism occupies a large part of the Byrranga Mountains, which extend over a distance of 1000 km from Dikson Island to the Laptev Sea (Fig. 8) (Bezzubtsev *et al*. 1983). Southern Taimyr is a Mesozoic fold belt and flood basalts are preserved there in synclines, mostly in the western part, whereas the basalt-related sills and dykes are abundant throughout the belt. The sills usually occur within Permian coal-bearing terrigenous deposits, sometimes dominating the host rocks (Bezzubtsev *et al*. 1983, 1986; Walderhaug *et al*. 2005).

The flood basalts or sills are visible on seismic profiles and were reached by deep boreholes in the Yenisey–Khatanga Basin (Fig. 8). This depression, also known as Pyasina–Khatanga Basin or Khatanga Basin, started subsiding in the Mesozoic and the subsidence continued until the Quaternary. In Early Triassic time flood basalts probably covered the entire area from Tunguska Basin and throughout southern Taimyr.

The sequence of trap emplacement across Taimyr falls into three phases. The first phase, the stratigraphically lowest portion, of the trap section is represented by interbedded tuff, lava and shale. The lavas are trachybasaltic and andesite–basaltic in composition (Bezzubtsev *et al*. 1986). Trap volcanic rocks erupted mostly subaerially, but also subaqueously. The second, main phase of emplacement is represented by tholeiitic flood basalts of 1000–3000 km thickness. These are missing from eastern Taimyr, where the entire volcanic section (about 300 m thick) is dominated by first-phase volcanic rocks, sills and dykes.

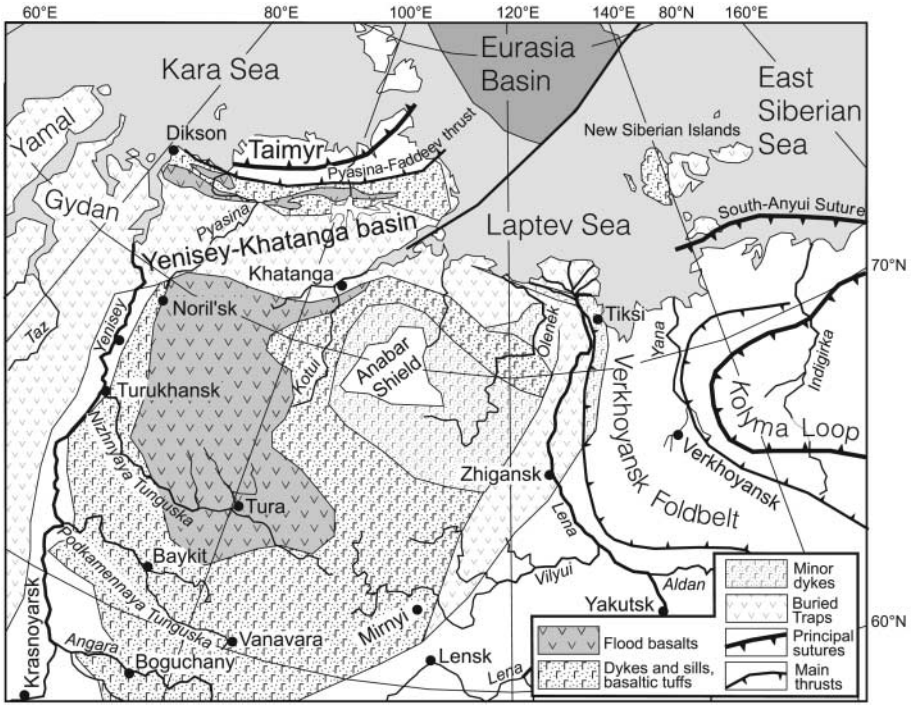

Fig. 8. Regional map of the Siberian trap province, compiled from multiple sources (Harkevich 1971; Bezzubtsev *et al*. 1983; Prokopiev *et al*. 2001, and others).

Some intrusions are differentiated and contain picritic, troctolitic and anorthositic zones (Bezzubtsev *et al*. 1986). Alkaline dolerite and gabbro have also been reported, but they are more typical of the second stage. The final phase of emplacement is represented by occasional trachyte and trachyrhyolite, which form the capping flows of basaltic plateaux up to 200 m thick. Alkalic intrusions are more abundant and include essexite, syenite and other exotic varieties (Bezzubtsev *et al*. 1986). In western Taimyr these rocks are dated at 249–241 Ma (Vernikovsky *et al*. 2003). These three stages of trap evolution have also been reported for other flood-basalt provinces (Sheth 1999; Jerram & Widdowson 2005; Ross *et al*. 2005). The Bel'kov Island trap magmatism is similar to the initial stage, which is characterized by prevalent phreatomagmatic eruptions and transitional–alkaline magma composition. Consequently, the Bel'kov Island magmatism belongs to the northeastern margin of the Siberian trap province and was probably emplaced during its initial stage.

Tectonic implications

If we assume that the New Siberian Islands belong to the Siberian continental flood basalt province, they must have been a part of Siberia in Early Triassic time. As indicated above, the most probable tectonic position of the western Anjou Islands is adjacent to eastern Taimyr, which was the northern foreland of the Siberian Platform in the Triassic (Bogdanov & Khain 1998). This is consistent with the similarity between the Palaeozoic deposits and fossil records in these two regions (Cherkesova 1975). Thus, an oceanic basin did not separate the Siberian Platform from the New Siberian carbonate platform in the Early Triassic. Kotel'ny Island and Bel'kov Island belonged to the same block, as both exhibit the same Palaeozoic section intruded by the same dolerites (Kos'ko *et al*. 1985).

Early and pre-Mesozoic Arctic tectonic reconstructions must take this into account. This especially concerns models implying that an oceanic basin separated the New Siberian carbonate platform from Siberia in Late Palaeozoic–Early Triassic time (Zonenshain *et al*. 1990; Drachev *et al*. 1998; Natal'in *et al*. 1999; Sokolov *et al*. 2002). In other words, the third and fourth positions described above for the western boundary of the 'rotational' terrane comprising the East Siberian shelf, Northern Chukotka and Arctic Alaska are not viable (namely, the proposal that places the suture or regional transform west of Bel'kov Island (line 3, Fig. 1) and the one implying that the New Siberian Islands were connected with northern Taimyr and Severaya Zemlya).

However, the geological affinities between the New Siberian carbonate platform and the Siberian Platform also need to be taken into account by those geologists who believe that the Bel'kov and Kotel'ny Islands do not belong to the East Siberian shelf–Northern Chukotka terrane (e.g. Rowley & Lottes 1988; Lawver *et al*. 2002). It is very likely that the New Siberian carbonate platform extended eastwards of Kotel'ny Island. We agree with Natal'in *et al*. (1999) that the New Siberian platform covered a significant portion of East Siberian shelf. Moreover, it is possible that the northern zone of the Siberian trap province did not stop at the New Siberian Islands, but possibly extended further eastward towards Chukotka. Tholeiitic dolerites and gabbro sills and dykes are abundant in Northern Chukotka (Natal'in 1984, Sukhov & Kazinskaya 1999) and it has been suggested that they represent Siberian traps (e.g. Gel'man 1963). It must be noted, however, that these igneous rocks are poorly studied and their age is not confidently known. Similar conclusions on the close relationship between Northern Chukotka and the Siberian Platform in the Triassic have been made recently based on detrital zircon (Miller *et al*. 2006). However, detailed discussion of the relationship between the New Siberian Islands and Northern Chukotka is beyond the scope of this paper, which focuses on the western half of the East Arctic tectonic problem and suggests that the continental massif including the western New Siberian Islands was attached to Siberia in the Early Mesozoic. This constrains the location of the New Siberian Islands within an Arctic tectonic framework prior to the Amerasia basin opening.

Conclusions

Mafic igneous rocks in the western New Siberian Islands represent subvolcanic intrusions of mantle-derived magma strongly modified by crustal contamination. Their U–Pb zircon age of 252 ± 2 Ma (95% confidence, MSWD $= 1.3$, $n = 9$), petrographic features and geochemical signatures are the same as those of Siberian trap magmatism. These data indicate that the western New Siberian Islands were a part of the Siberian trap province. The Siberian intraplate volcanic activity at the Permian–Triassic boundary was short-lived and occurred over a large region that included the western New Siberian Islands. This suggests that the western New Siberian Islands were not an exotic terrane separated from Siberia by an ocean in Early Mesozoic time, but were a part of the Siberian Platform. This inference should be taken into account in Mesozoic Arctic plate tectonic reconstructions.

This work was funded by the Russian Foundation for Basic Research (project no. 05-05-64028), EU INTAS Grant (01-0762 NEMLOR), Earth-Science programme no. 14 of RAS and the Swedish Research Council (grant 621-2004-5326). Thanks go to M. J. Whitehouse and the NORDSIM facility. The NORDSIM facility is funded by the research councils of Denmark, Norway, Sweden, the Geological Survey of Finland, and the Swedish Museum of Natural History. This is NORDSIM publication 169. We also thank R. Scott, L. Lawver and R. Ernst for their constructive reviews, and D. Peate for careful editorial handling, which contributed to the improvement of the manuscript.

References

Al'Mukhamedov, A.I., Medvedev, A.Ya. & Kirda, N.P. 1999. Comparative analysis of geodynamic setting of the Permo-Triassic magmatism in East Siberia and West Siberia. *Russian Geology and Geophysics*, **40**, 1550–1561.

Arndt, N.T., Czamanske, G.K., Wooden, J.L. & Fedorenko, V.A. 1993. Mantle and crustal contributions to continental flood volcanism. *Tectonophysics*, **223**, 39–52.

Benton, M.J. & Twitchett, R.J. 2003. How to kill (almost) all life: the end-Permian extinction event. *Trends in Ecology and Evolution*, **18**, 358–365.

Bezzubtsev, V.V., Malich, N.S., Markov, F.G. & Pogrebitsky, Yu.E. (eds) 1983. *Geological Map of Mountainous Taimyr, scale 1:500 000*. Krasnoyarskgeologia.

Bezzubtsev, V.V., Zalyaleev, R.Sh., Goncharov, Yu.I. & Sakovich, A.B. 1986. *Geological Map of Mountainous Taimyr, scale 1:500 000. Explanatory Note*. Krasnoyarskgeologia.

Bogdanov, N.A. & Khain, V.E. (eds) 1998. *Tectonic map of the Kara and Laptev Seas and North Siberia, scale 1:2 500 000*. Russian Academy of Sciences, Institute of the Lithosphere of Marginal Seas, Moscow.

Cherkesova, S.V. 1975. Comparative characteristics of the Lower–Middle Devonian deposits of northwestern Kotel'ny Island and other Arctic regions. *In:* Vol'nov, D.A. (ed.) *Geology and Mineral Deposits of New Siberian and Wrangel Islands*. NIIGA, Leningrad, 22–27 (in Russian).

Dalrymple, B.G., Czamanske, G.K., Fedorenko, A., Simonov, O.N., Lanphere, M.A. & Likhachev, A.P. 1995. A reconnaisance $^{40}Ar/^{39}Ar$ geochronological study of ore-bearing and related rocks, Siberian Russia. *Geochimica et Cosmochimica Acta*, **59**, 2071–2083.

Dobretsov, N.L. 2005. Large igneous provinces of Asia (250 Ma): Siberian and Emeishan traps (plateau basalts) and associated granitoids. *Russian Geology and Geophysics*, **46**, 847–868.

Drachev, S.S., Savostin, L.A., Groshev, V.G. & Bruni, I.E. 1998. Structure and geology of the continental shelf of the Laptev Sea, Eastern Russian Arctic. *Tectonophysics*, **298**, 357–393.

Garbe-Schonberg, C.-D. 1993. Simultaneous determination of thirty-seven trace elements in twenty-eight international rock standards by ICP-MS. *Geostandards Newsletter*, **17**, 81–97.

Gel'man, M.L. 1963. The Triassic dolerite suite of Anyui zone (Chukotka). *Russian Geology and Geophysics*, **4**, 127–134 (in Russian).

Grantz, A., Clark, D.L., Phillips, R.L. & Srivastava, S.P. 1998. Phanerozoic stratigraphy of Northwind Ridge, magnetic anomalies in the Canada basin, and geometry and timing of rifting in the Amerasia basin, Arctic Ocean. *Geological Society of America Bulletin*, **110**, 801–820.

Harkevich, D.S. (ed.) 1971. *The map of igneous complexes of USSR, scale 1:2 500 000*. VSEGEI, Moscow (in Russian).

Hawkesworth, C.J., Lightfoot, P.C., Fedorenko, V.A., Blake, S., Naldrett, A.J., Doherty, W. & Gorbachev, N.S. 1995. Magma differentiation and mineralization in the Siberian continental flood basalts. *Lithos*, **34**, 61–88.

Hergt, J.M., Peate, D.W. & Hawkesworth, C.J. 1991. The petrogenesis of Mesozoic Gondwana low-Ti flood basalts. *Earth and Planetary Science Letters*, **105**, 134–148.

Jerram, D.A. & Widdowson, M. 2005. The anatomy of Continental Flood Basalt Provinces: geological constraints on the processes and products of flood volcanism. *Lithos*, **79**, 385–405.

Kamo, S.L., Czamanske, G.K. & Krogh, T.E. 1996. A minimum U–Pb age for Siberian flood-basalt volcanism. *Geochimica et Cosmochimica Acta*, **60**, 3505–3511.

Kamo, S.L., Czamanske, G.K., Amelin, Y., Fedorenko, V.A., Davis, D.W. & Trofimov, V.R. 2003. Rapid eruption of Siberian flood-volcanic rocks and evidence for coincidence with the Permian–Triassic boundary and mass extinction at 251 Ma. *Earth and Planetary Science Letters*, **214**, 75–91.

Kos'ko, M.K. & Nepomiluev, V.F. 1980. *State geological map of the USSR, 1:200 000 scale. Sheet S-53-IV, V, VI*. VSEGEI, Leningrad (in Russian).

Kos'ko, M.K. & Trufanov, G.V. 2002. Middle Cretaceous to Eopleistocene sequences on the New Siberian Islands: an approach to interpret offshore seismic. *Marine and Petroleum Geology*, **19**, 901–919.

Kos'ko, M.K., Bondarenko, N.S. & Nepomiluev, V.F. 1985. *State geological map of the USSR, 1:200 000 scale. Sheets T-54-XXXI, XXXXII, XXXXIII; S-53-IV, V, VI, XI,XII; S-54-VII,VIII, IX, XIII, XIV, XV. Explanatory note*. Ministry of Geology, Moscow (in Russian).

Kos'ko, M.K., Cecile, M.P., Harrison, J.C., Ganelin, V.G., Khandoshko, N.V. & Lopatin, B.G. 1993. Geology of Wrangel Island, between Chukchi and East Siberian seas, northeastern Russia. *Geological Survey of Canada Bulletin, Report*, 461.

Kuzmichev, A. 2004. Subvolcanic dykes and peperites in western Bel'kov Island—a backcountry of the Siberian trap province on the New Siberian Islands. *Norsk Geologisk Forening*, **2**, 83–85.

Kuzmichev, A. & Bogdanov, N. 2003. Where does the South Anyui suture go to in the New Siberian Islands and Laptev Sea?: implication to the rotational hypothesis of the Amerasia Basin opening. EGS–AGU–EUG Joint Assembly. *Geophysical Research Abstracts*, **5**, abstract EAE03-A-05165.

Kuzmichev, A.B., Sklyarov, E.V. & Barash, I.G. 2005. Pillow basalts and blueschists on Bol'shoi Lyakhovsky Island (the New Siberian Islands)—fragments of the South Anyui oceanic lithosphere. *Russian Geology and Geophysics*, **46**, 1367–1381.

Kuzmichev, A.B., Soloviev, A.V., Gonikberg, V.E., Shapiro, M.N. & Zamzhitskii, O.V. 2006. Mesozoic syncollision siliciclastic sediments of the Bol'shoi Lyakhov Island (New Siberian Islands). *Stratigraphy and Geological Correlation*, **14**, 30–48.

Lawver, L.A., Grantz, A. & Gahagan, L.M. 2002. Plate kinematic evolution of the present Arctic region since the Ordovician. *In:* Miller, E.L., Grantz, A. & Klemperer, S.L. (eds) *Tectonic Evolution of the Bering Shelf–Chukchi Sea–Arctic Margin and Adjacent Landmasses*. Geological Society of America, Special Papers, **360**, 333–358.

Layer, P.W., Newberry, R., Fujita, K., Parfenov, L., Trunilina, V. & Bakharev, A. 2001. Tectonic setting of the plutonic belts of Yakutia, northeast Russia, based on $^{40}Ar/^{39}Ar$ geochronology and trace element geochemistry. *Geology*, **29**, 167–170.

Lightfoot, P.C., Naldrett, A.J., Gorbachev, N.S., Doherty, W. & Fedorenko, A. 1990. Geochemistry of the Siberian trap of the Noril'sk area, USSR, with implications for the relative contributions of crust and mantle to flood basalt magmatism. *Contributions to Mineralogy and Petrology*, **104**, 631–644.

Lightfoot, P.C., Hawkesworth, C.J., Hergt, J., Naldrett, A.J., Gorbachev, N.S., Fedorenko, A. & Doherty, W. 1993. Remobilization of the continental lithosphere by a mantle plume: major-, trace-element, and Sr-, Nd- and Pb-isotopic evidence from picritic and tholeiitic lavas of the Noril'sk district, Siberia. *Contributions to Mineralogy and Petrology*, **114**, 171–188.

Miller, E.L., Toro, J. & Gehrels, G. *et al.* 2006. New insights into Arctic paleogeography and tectonics from U–Pb detrital zircon geochronology. *Tectonics*, **25**, paper TC3013.

Natal'in, B.A. 1984. *Early Mesozoic Eugeosyncline Systems of Northern Pacific Frame*. Nauka, Moscow (in Russian).

Natal'in, B.A., Amato, J.M., Toro, J. & Wright, J.E. 1999. Palaeozoic rocks of Northern Chukotka Peninsula, Russian Far East: implications for the tectonics of the Arctic Region. *Tectonics*, **18**, 977–1003.

Parfenov, L.M., Natapov, L.M., Sokolov, S.D. & Tsukanov, N.V. 1993. Terranes and accretionary tectonics of northeastern Russia. *Geotectonics*, **1**, 68–78 (in Russian).

Peate, D.W. & Hawkesworth, C.J. 1996. Lithospheric to asthenospheric transition in Low-Ti basalts from southern Parana, Brazil. *Chemical Geology*, **127**, 1–24.

Pik, R., Deniel, C., Coulon, C., Yirgu, G. & Marty, B. 1999. Isotopic and trace element signatures of Ethiopian flood basalts: evidence for plume–lithosphere interactions. *Geochimica et Cosmochimica Acta*, **63**, 2263–2279.

Prokopiev, A.V., Parfenov, L.M., Tomshin, M.D. & Kolodesnikov, I.I. 2001. The cover of Siberian Platform and adjacent thrust-and-fold belts. *In:* Parfenov, L.M. & Kuz'min, M.I. (eds) *Tectonics, Geodynamics and Metallogeny of the Sakha Republic (Yakutia)*. MAIK 'Nauka/Interperiodica', Moscow, 113–155 (in Russian).

Reichow, M.K., Saunders, A.D., White, R.V., Pringle, M.S., Al'Mukhamedov, A.I., Medvedev, A.I. & Kirda, N.P. 2002. $^{40}Ar/^{39}Ar$ dates from the West Siberian Basin: Siberian flood basalt province doubled. *Science*, **296**, 1846–1849.

Reichow, M.K., Saunders, A.D., White, R.V., Al'Mukhamedov, A.I. & Medvedev, A.Ya. 2005. Geochemistry and petrogenesis of basalts from the West Siberian Basin: an extension of the Permo-Triassic Siberian Traps, Russia. *Lithos*, **79**, 425–452.

Renne, P.R. & Basu, A.R. 1991. Rapid eruption of the Siberian traps flood basalts at the Permo-Triassic boundary. *Science*, **253**, 176–179.

Renne, P.R., Zichao, Z., Richards, M.A., Black, M.T. & Basu, A.R. 1995. Synchrony and causal relations between Permian–Triassic boundary crisis and Siberian flood volcanism. *Science*, **269**, 1413–1416.

Ross, P.-S., Ukstins Peate, I. & McClintock, M.K. *et al.* 2005. Mafic volcaniclastic deposits in flood basalt provinces: a review. *Journal of Volcanology and Geothermal Research*, **145**, 281–314.

Rowley, B.R. & Lottes, A.L. 1988. Plate-kinematic reconstructions of the North Atlantic and Arctic: Late Jurassic to present. *Tectonophysics*, **155**, 73–120.

Sharma, M., Basu, A.R. & Nesterenko, G.V. 1991. Nd–Sr isotopes, petrochemistry, and origin of the Siberian flood basalts, USSR. *Geochimica et Cosmochimica Acta*, **55**, 1183–1192.

Sharma, M., Basu, A.R. & Nesterenko, G.V. 1992. Temporal Sr-, Nd- and Pb-isotopic variations in the Siberian flood basalts: implications for the plume-source characteristics. *Earth and Planetary Science Letters*, **113**, 365–381.

Sheinman, Yu.M. 1947. The new petrographic province at the northern Siberian Platform. *Izvestia of Academy of Sciences of USSR, Geological Series*, **1**, 123–134 (in Russian).

Sheth, H.C. 1999. A historical approach to continental flood basalt volcanism: insights into pre-volcanic rifting, sedimentation, and early alkaline magmatism. *Earth and Planetary Science Letters*, **168**, 19–26.

Sokolov, S.D., Bondarenko, G.Ye., Morozov, O.L., Shekhovtsov, V.A., Glotov, S.P., Ganelin, A.V. & Kravchenko-Berezhnoy, I.R. 2002. South Anyui suture, northeast Arctic Russia: facts and problems. *In:* Miller, E.L., Grantz, A. & Klemperer, S. (eds) *Tectonic Evolution of the Bering Shelf–Chukchi Sea–Arctic Margin and Adjacent Landmasses*. Geological Society of America, Special Papers, **360**, 209–224.

Spector, V.B., Andrusenko, A.M., Dudko, E.A. & Kareva, N.F. 1981. Continuation of the South Anyui suture in the Primorsky lowland. *Doklady Akademii Nauk SSSR*, **260**, 1447–1450 (in Russian).

Stacey, J. & Kramers, J. 1975. Approximation of terrestrial lead isotope evolution by a two-stage model. *Earth and Planetary Science Letters*, **26**, 207–221.

Steiger, R.H. & Jäger, E. 1977. Subcommission on geochronology: convention on the use of decay constants in geo- and cosmochronology. *Earth and Planetary Science Letters*, **36**, 359–362.

Sukhov, K.S. & Kazinskaya, G.I. (compilers) 1999. *State Geological Map of Russian Federation, scale 1:1 000 000 (new series). Sheet R-(60)-2. Explanatory note*. VSEGEI, St. Petersburg (in Russian).

Sun, S.-s. & McDonough, W.F. 1989. Chemical and isotopic systematics of oceanic basalts: implications for mantle composition and processes. *In:* Saunders, A.D. & Norry, M.J. (eds) *Magmatism in the Ocean Basins*. Geological Society, London, Special Publications, **42**, 313–345.

Trufanov, G.V., Belousov, K.N. & Nepomiluev, V.F. 1986. *State geological map of the USSR, 1:200 000 scale. Sheets T-54-XXXIV, XXXV, XXXVI; T-56-XXXIII; S-54-IV, V, VI, X, XI, XII; S-55-I, II, III, IV, V, VI, VII, VIII, IX, X, XI, XII; S-56-III, VII. Explanatory note*. Ministry of Geology, Moscow (in Russian).

Unksov, V.F. 1934. *Traps at Una, Chuna, Taseeva Rivers (Eastern Siberia)*. Transactions, Council on Resources, Siberian Series, **18 (in Russian)**.

Venkatesan, T.R., Kumar, A., Gopalan, K. & Al'Mukhamedov, A.I. 1997. ^{40}Ar–^{39}Ar age of Siberian basaltic volcanism. *Chemical Geology*, **138**, 303–310.

Vernikovsky, V.A., Pease, V.L., Vernikovskaya, A.E., Romanov, A.P., Gee, D.G. & Travin, A.V. 2003. First report of early Triassic A-type granite and syenite intrusions from Taimyr: product of the northern Eurasian superplume? *Lithos*, **66**, 23–36.

Vol'nov, D.A., Lopatin, B.G., Sorokov, D.S., Kos'ko, M.K. & Dorofeev, V.K. 1999. *State Geological Map of Russian Federation, scale 1:1 000 000 (New Series). Sheet S-53-55-New Siberian Islands. Explanatory Notes*. VSEGEI, St. Petersburg (in Russian).

Walderhaug, H.J., Eide, E.A., Scott, R.A., Inger, S. & Golionko, E.G. 2005. Palaeomagnetism and $^{40}Ar/^{39}Ar$ geochronology from the South Taimyr igneous complex, Arctic Russia: a Middle–Late Triassic magmatic pulse after Siberian flood-basalt volcanism. *Geophysical Journal International*, **163**, 501–517.

Walker, R.J., Morgan, J.W., Horan, M.F., Czamanske, G.K., Krogstad, E.J., Fedorenko, A. & Kunilov, E. 1994. Re–Os-isotopic evidence for an enriched-mantle source for the Noril'sk-type, ore-bearing intrusions, Siberia. *Geochimica et Cosmochimica Acta*, **58**, 4179–4197.

Whitehouse, M., Claesson, S., Sunde, T. & Vestin, J. 1997. Ion-microprobe U–Pb zircon geochronology and correlation of Archaean gneisses from the Lewisian Complex of Gruinard Bay, northwestern Scotland. *Geochimica et Cosmochimica Acta*, **61**, 4429–4438.

Whitehouse, M., Kamber, B. & Moorbath, S. 1999. Age significance of U–Th–Pb zircon data from early Archaean rocks of west Greenland—a reassessment based on combined ion-microprobe and imaging studies. *Chemical Geology*, **160**, 201–224.

Wooden, J.L., Czamanske, G.K. & Fedorenko, V.A. *et al.* 1993. Isotopic and trace-element constraints on mantle and crustal contributions to Siberian continental flood basalts, Noril'sk area, Siberia. *Geochimica et Cosmochimica Acta*, **57**, 3677–3704.

Zonenshain, L.P., Kuzmin, M.I. & Natapov, L.M. 1990. *Geology of the USSR: a plate tectonic synthesis*. American Geophysical Union, Geodynamics Series, **21**.

Received 14 June 2006; revised typescript accepted 30 January 2007.
Scientific editing by David Peate